Proceedings of the tenth international conference on liquid and amorphous metals,
Dortmund, 1998, J. Non-Crystal. Solids, in press.

Structural Studies of Expanded Fluid Mercury Using Synchrotron Radiation

K. Tamura, M. Inui, I. Nakaso, Y. Oh'ishi, K. Funakoshi§ and W. Utsumi§§

Faculty of Integrated Arts and Sciences, Hiroshima University, Higashi-Hiroshima 739-8521, Japan
§*Japan Synchrotron Radiation Research Institute, Kamigori 679-5198, Japan*
§§*The Japan Atomic Energy Research Institute, Kamigori 679-5198, Japan*

Abstract

The energy-dispersive x-ray diffraction measurements using synchrotron radiation at SPring-8 for expanded fluid Hg were carried out for the first time in the density range from the liquid to the dense vapour region including the metal-nonmetal transition region. Densities ranged from 13.6 to 1.9 gcm^{-3}. We obtained the structure factor $S(k)$ and the pair distribution functions $g(r)$. The density variations of the obtained interatomic distance r_1 and coordination number N_1 were discussed in relation to the M-NM transition in fluid Hg.

1 Introduction

Liquid Hg is transformed into an insulating state when it is expanded to the liquid-gas critical point (critical data of Hg [1]: $T_c = 1478$ °C, $p_c = 1673$ bar, $d_c = 5.8$ gcm^{-3}). Many investigations have been made considering the metal-nonmetal (M-NM) transition in fluid Hg. The first indication of the M-NM transition was found in the electrical conductivity and thermopower data obtained by Hensel and Frank[2]. Measurements of physical properties such as electrical conductivity [3]–[5], thermopower [3],[6]–[8], Hall coefficient [9], optical reflectivity [10, 11], optical absorption coefficient [12, 13] and nuclear magnetic resonance [14] indicate that, as the density is reduced, the M-NM transition starts to occur at a density of about 9 gcm^{-3}.

Theoretical attempts have been made to understand the M-NM transition. Devillers and Ross [15] applied a pseudopotential method to calculate the energy bands for crystalline Hg with expanded bcc, fcc and rhombohedral structures. Band-structure calculations for such a uniformly expanded crystalline Hg were carried out by many others [16, 17]. An alternative approach by Mattheis and Warren [18] assumed that the nearest-neighbor distance was constant, so the density variation in expanded fluid Hg was due entirely to the changes in the coordination number.

It is obvious that the information on the atomic arrangement of expanded fluid Hg is quite important for understanding the M-NM transition. However, the diffraction experiments for expanded fluid Hg are not easy because the critical pressure is 1673 bar. Recently Tamura and Hosokawa measured x-ray diffraction using an in-house x-ray source for expanded liquid Hg in the metallic region and also up to the critical region [19]–[21]. They obtained information about the first neighbour distance, r_1, which remains almost constant while the first neighbouring coordination number, N_1, decreases substantially and almost linearly with decreasing density in the metallic region. It is important to study how liquid Hg expands with further decrease of density, beyond the M-NM transition region to the dense vapour region.

In this paper we present results of x-ray diffraction measurements using a synchrotron radiation at the super-photon ring operating at 8 GeV (SPring-8) in Japan, extending from the liquid to the dense vapour region beyond the liquid-vapour critical point, which enable us to get more precise information about the atomic configuration.

2 Experiment

We have performed energy-dispersive x-ray diffraction measurements for expanded fluid Hg using a synchrotron radiation on the BL-04B1 at SPring-8. In the energy-dispersive method, white x-rays were used as the primary beam, and the scattered photons were detected and energy-analyzed by a solid state detector (SSD). This technique has been employed in our in-house structural studies of expanded fluids [19]–[24]. The storage ring at SPring-8 was operated at 8 GeV with 20 mA during the present experiment. White x-rays were generated through the bending magnet ranging in energy to 150 keV.

The experimental conditions of temperatures to 1520 °C, and pressures to 1765 bar, were achieved with an internally heated high-pressure vessel made of a super-high-tension steel. The design of the high pressure vessel is almost the same as that of the previous one [24] and the construction of the vessel is described in the literature [25]. Helium gas was used as a pressure transmitting medium. Expanded fluid Hg must be contained in a cell made of a special material being transparent to x-rays and resistant to chemical corrosion by hot fluid Hg. A single-crystal sapphire cell was developed for this purpose, the details of which are described in the literature [24].

The diffracted x-ray photons from expanded fluid Hg at high temperatures and pressures were collected at the scattering angle 2θ of 5, 10, 20, and 33°. The spectrum used for the analysis was in the energy region 16 to 60 keV because the fluorescence peak appeared at larger energy. To obtain the structure factor, $S(k)$, of expanded fluid Hg from the experimental scattering intensity, several data corrections had to be made. The details of the data analysis were described in the literature [21, 26].

3 Results

We have carried out x-ray diffraction measurements for expanded fluid Hg in the temperature and pressure ranges to 1520 °C and 1765 bar along the saturated vapor-pressure curve and with densities ranging from 13.6 to 1.9 gcm^{-3}. Figure 1 shows the $S(k)$ for expanded fluid Hg in the different temperatures and pressures using the cell with the sample thickness of 60 μm. Dots represent the experimental data and the full curves show the Fourier-transforms of $g(r)$ in Fig. 2.

Figure 2 shows the $g(r)$, the Fourier-transforms of $S(k)$, of fluid Hg. The transform of the $S(k)$ function requires data from $k = 0$ to ∞. The $S(k)$'s in the region between 0 and 1.0 Å^{-1} were estimated by interpolating the $S(0)$'s and $S(k)$ above 1.0 Å^{-1}, where the $S(0)$'s were calculated using the experimentally obtained isothermal compressibility of expanded fluid Hg [1, 4].

The data for $g(r)$ at 25 °C and 394 bar have several features; the first peak has an asymmetric shape, the first minimum is invariant in the region from 4 to 5 Å and the second peak is rather small. The data for $g(r)$ at 25 °C and 394 bar are in agreement with the previous data at normal condition [27]. With increasing temperature and pressure, with decreasing density, the long-range oscillation of $g(r)$ diminishes. The broadening of the first peak gradually occurs but no change of the peak position is observed and the asymmetry of the first peak remains even at temperatures and pressures up to 1480 °C and 1765 bar, respectively, with density of 8.0 gcm^{-3}. It should be noted that the shape and the position of first peak changes when the density further decreases and the dense vapour region is approached. The amplitude of the second peak decreases with increasing temperature and pressure.

4 Discussion

To obtain the definite coordination number, N_1, from the $g(r)$ pattern of the non-crystalline state we employed two different methods to define and to integrate the first-neighbor peak [28]. The first (method A) is the method of integrating $4\pi r^2 \rho_0 g(r)$ up to the first maximum of $g(r)$, r_1, and taking twice the integral, where ρ_0 denotes the average number density of Hg. The second (method B) is a method of taking the asymmetry of the first-neighbor peak into account. In method B, a tangential straight line is drawn from the first peak position, r_{max}, towards the first minimum of $4\pi r^2 \rho_0 g(r)$. The triangle area below the tangent line is regarded as that due to the penetration of the second-neighbors, and is subtracted.

The coordination numbers, N_1, obtained by these calculations are plotted in figure 3 as a function of density. The nearest-neighbor distance, r_1, is also shown as a function of density at the bottom of figure 3. In the figure we plot the data obtained by using the cells with sample thickness of 30 and 60 μm. As is seen in figure 3, N_1 decreases linearly with decreasing density in the metallic region, whatever method is employed. On the contrary, r_1 in the metallic region remains almost unchanged with decreasing density within the accuracy of the present experiment. From these results we conclude that the volume-expansion of liquid Hg in the metallic region is not a uniform expansion with a fixed coordination number, but is caused by a decrease of coordination number with a fixed nearest-neighbor distance. The atomic arrangement of metallic liquid Hg would be changed with decreasing density essentially in the way that Hg atoms are taken away one by one from the random array with a constant nearest-neighbor distance. When the M-NM transition is approached from the high density side, i.e., around 10 gcm^{-3}, however, another deviation from the linearity of N_1 as a function of density is observed. In addition, r_1 starts to increase. When the dense vapour region is approached with further decreasing density, r_1 increases. The r_1 seems to approach the interatomic distance $\sim$ 3.3 Å of Hg dimers in the rarefied vapour, obtained from optical measurements [30]. We suggest that the gross feature of the density variation of N_1 and r_1 in figure 3 shows that there exist three different regions in the density, that is, the metallic region from 13.6 to about 10 g/cm^3, the M-NM transition region from 10 to the critical density of about 6 g/cm^3 and the dense vapour region.

As mentioned in the previous section several band structure calculations were carried out for the hypothetical forms of crystalline Hg with uniformly expanded lattice constants in the low density limit [15]–[17]. The present experimental results for fluid Hg, however, differ. One of the approaches whose principle was consistent with the present experimental results was that of Mattheis and Warren [18]. They assumed that the nearest-neighbor distance was constant, so the density variation in expanded fluid Hg was due entirely to the changes in the coordination number. They performed a series of augmented-plane-wave calculations for crystalline Hg with fcc, bcc, sc, and diamond structures with a fixed nearest-neighbor distance. They found that the trend of the density dependence of the theoretically calculated density of states (DOS) with the character of 6s wave function is in good agreement with that of the Knight shift in the density range down to about 9.5 gcm^{-3} by assuming that N_1 of liquid Hg near the triple point was 10, and decreased linearly with decreasing density. However, their hypothetical crystal with diamond structure with $N_1 = 4$, which corresponds to $\rho = 5.4$ gcm^{-3} by the interpretation of Warren and Hensel [31] using revised density data, indicates a semimetallic DOS, and it was found necessary to increase the lattice constant by 1 % to fully open a gap.

Franz [32] proposed a model that produces a real gap at the correct density of 9 gcm^{-3}. The model was also based on the assumption of a linear decrease in average coordination number with decreasing density, but in addition it takes into account the fact that the actual local coordination numbers would be distributed randomly over a range around the mean N_1. It was assumed from the previous calculations [18] that for $N_1 = 4$ a gap is just before opening, while for $N_1 = 3$ a gap should exist. Franz postulated that the local gap of atoms with $N_1 = 3$ prevents electrons from hopping onto it from neighboring atoms, and such a vacancy against the transport propagates throughout the liquid at a well-defined mean-density, creating a real gap in the total DOS. The density of the percolation threshold or the M-NM transition density obtained was about 9 gcm^{-3}. The results based on the model suggest that fluctuations of the coordination number affect the M-NM transition in fluid Hg.

Recently, Kresse and Hafner [33] made a theoretical investigation on the density variation of the structural and electronic properties of fluid Hg using an ab initio density-functional molecular dynamics method. They found that a single-particle gap between the 6s and 6p bands opens at a density of about 8.8 gcm^{-3}. They could reproduce the volume expansion in fluid Hg, which does not result in an increase of the mean interatomic distance, r_1, but in a decrease of the average coordination number, N_1. In addition, the asymmetry of the first peak in $g(r)$ was reproduced in their calculated results over the whole density range.

We have so far discussed the density variation of the first neighbour coordination in relation to the M-NM transition in fluid Hg. The asymmetry of the first peak remains even at temperatures and pressures up to 1480 °C and 1765 bar, respectively, with density of 8.0 gcm^{-3}. The asymmetry may indicate that there exist two sites in the first coordination shell. The changes of the coordination number and the position of these sites in the first neighbour shell must play a role in the M-NM transition.

In the dense vapour region, we can see in figure 2 that the first peak , the shape of which is changed compared with those in the metallic region, remains resolved but the second-neighbor correlation is almost lost. We suggest that this effect is due to small clusters such as Hg dimers ($N_1 = 1$), triangles ($N_1 = 2$), or tetrahedrons ($N_1 = 3$) which may exist near the critical range.

5 Conclusion

From x-ray diffraction results obtained using synchrotron radiation at SPring-8, we conclude that the volume-expansion of liquid Hg in the metallic region is not a uniform expansion with a fixed coordination number, but is caused by a decrease of coordination number with a fixed nearest-neighbor distance. When the M-NM transition is approached another deviation from the linearity of N_1 as a function of density is observed. In addition, r_1 starts to increase. When the dense vapour region is approached, r_1 increases. The r_1 seems to approach the interatomic distance of Hg dimers in the rarefied vapour. It was found that from the density variations of N_1 and r_1 there exist three characteristic density regions, that is, the metallic, M-NM transition and the dense vapour regions in which different behaviours in the structural change were clearly observed.

Acknowledgments

The authors are grateful to Professor S. Hosokawa for valuable discussions and Dr. Y. Sakaguchi for his technical assistance. Kobe Steel Co., Ltd., High Pressure System Co., Ltd. and Rigaku Co., Ltd. are acknowledged for the technical supports during the present experiment. This work is partly supported by the Grant-in-Aid for Scientific Research Fund from the Ministry of Education, Science and Culture of Japan, and Toray Science Foundation.

References

[1] W. Gözlaff, G. Schönherr, and F. Hensel, *Z. Phys. Chem.* NF **156** (1988) 219, W. Gözlaff, *PhD Thesis, University of Marburg* (1988).

[2] F. Hensel and E. U. Frank, *Ber. Bunsenges. Phys. Chem.* **70** (1966) 1154.

[3] R. W. Schmutzler and F. Hensel, *Ber. Bunsenges. Phys. Chem.* **76** (1972) 53.

[4] G. Schönherr, R. W. Schmutzler, and F. Hensel, *Philos. Mag.* B **40** (1976) 411

[5] M. Yao and H. Endo, *J. Phys. Soc. Jpn.* **51** (1982) 966.

[6] L. J. Duckers and R. G. Ross, *Phys. Lett.* A **38** (1972) 291.

[7] F. E. Neale and N. E. Cusack, *J. Phys.* F **9** (1979) 85.

[8] M. Yao and H. Endo, *J. Phys. Soc. Jpn.* **51** (1982) 1504.

[9] U. Even and J. Jortner, *Philos. Mag.* **25** (1972) 715; *Phys. Rev.* B **8** (1973) 2536.

[10] H. Ikezi, K. Schwarzenegger, A. L. Simons, A. L. Passner, and S. L. McCall, *Phys. Rev.* B **18** (1978) 2494.

[11] W. Hefner, R. W. Schmutzler, and F. Hensel, *J. Phys. Paris* **41** (1980) C8-62.

[12] H. Uchtmann and F. Hensel, *Phys. Lett.* **53A** (1975) 239; H. Uchtmann, U. Brusius, M. Yao, and F. Hensel, *Z. Phys. Chem.* NF **156** (1988) 151.

[13] M. Yao, K. Takehana and H. Endo, *J. Non-Cryst. Solids* **156-158** (1993) 807.

[14] U. El-Hanany and W. W. Warren, Jr., *Phys. Rev. Lett.* **34** (1975) 1276.

[15] M. A. C. Devillers and R. G. Ross, *J. Phys.* F **5** (1975) 73.

[16] H. Overhof, H. Uchtmann and F. Hensel, *J. Phys.* F **6** (1976) 523.

[17] P. Fritzson and K. -F. Berggren, *Solid State Commun.* **19** (1976) 385.

[18] L. F. Mattheis and W. W. Warren, Jr., *Phys. Rev.* B **16** (1977) 624.

[19] S. Hosokawa, T. Matsuoka and K Tamura, *J. Phys.: Condens. Matter* **3** (1991) 4443.

[20] K. Tamura and S. Hosokawa, *J. Phys. Paris IV - Colloque C5* **1** (1991) 39.

[21] K. Tamura and S. Hosokawa, *Phys. Rev.* B **58** (1998) 9030.

[22] K. Tamura, *J. Non-cryst. Solids* **117/118** (1990) 450.

[23] K. Tamura and S. Hosokawa, *Ber. Bunsenges. Phys. Chem.* **96** (1992) 681.

[24] K. Tamura, M. Inui and S. Hosokawa, *Rev. Sci. Instr.* in press.

[25] K. Tamura, M. Inui, I. Nakaso, Y. Oh'ishi, K. Funakoshi and W. Utsumi, J. Phys.: Condens. Matter, in press.

[26] K. Nishikawa and T. Iijima, *Bull. Chem. Soc. Jpn.* **57** (1984) 1750.

[27] L. Bosio, R. Cortes and C. Segaud, *J. Chem. Phys.* **71** (1979) 3595.

[28] C. J. Pings, *in Physics of simple liquids* ed. H. N. V. Temperley, J. S. Rowlinson, and G. S. Rushbrooke (North Holland, Amsterdam, 1968) 405-411.

[29] R. F. Mehl and C. S. Barrett, *Trans. A.I.M.E.* **89** (1930) 575.

[30] J. G. Winans and M. P. Heitz, *Z. Phys.* **133** (1952) 291; ibid. **135** (1953) 406.

[31] W. W. Warren, Jr. and F. Hensel, *Phys. Rev.* B **26** (1982) 5980.

[32] J. R. Franz, *Phys. Rev. Lett.* **57** (1986) 889.

[33] G. Kresse and J. Hafner, *Phys. Rev.* B **55** (1997) 7539.

Figure Captions

Figure 1	Structure factor $S(k)$ for expanded fluid Hg in the temperature and pressure ranges up to 1520 °C and 1765 bar along the saturated vapour-pressure curve. Temperature, pressure and density are indicated at the upper right hand side of each of the data points. The dots represent the experimental data and the full curves show the Fourier-transforms of $g(r)$ in figure 2.
Figure 2	Pair distribution functions $g(r)$ for expanded fluid Hg. Temperature, pressure and density are indicated at the upper right hand side of each of the data curves.
Figure 3	The coordination number N_1 and the nearest-neighbor distance r_1 of expanded fluid Hg as a function of density. Circles and triangles denote N_1 obtained using methods A and B, respectively (see text). Squares show the variation of r_1. Empty and full symbols indicate the data obtained using the cells with the sample thickness of 30 and 60 μm, respectively.

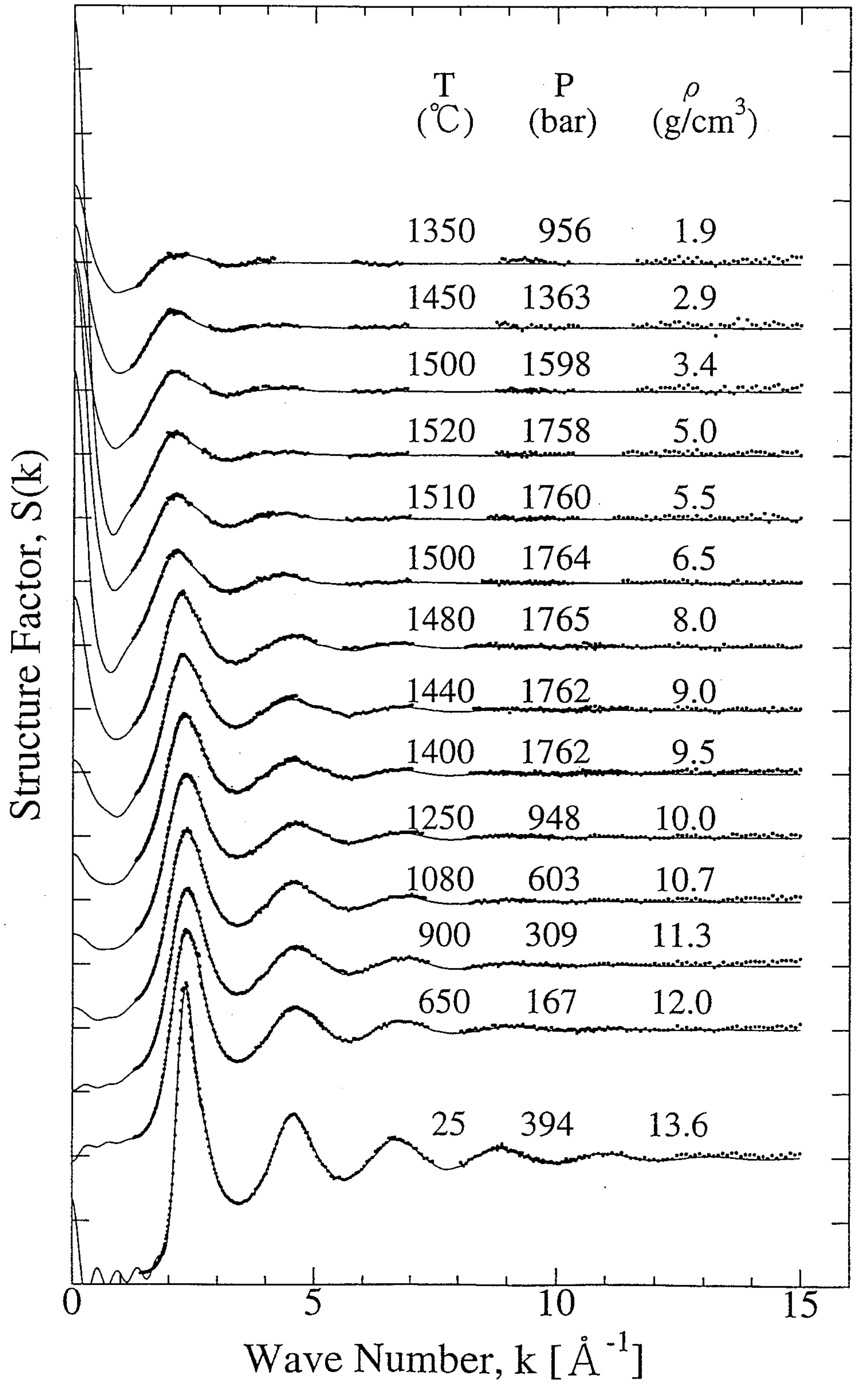
T (℃)
P (bar)
ρ (g/cm3)
1350 956 1.9
1450 1363 2.9
1500 1598 3.4
1520 1758 5.0
1510 1760 5.5
1500 1764 6.5
1480 1765 8.0
1440 1762 9.0
1400 1762 9.5
1250 948 10.0
1080 603 10.7
900 309 11.3
650 167 12.0
25 394 13.6
Structure Factor, S(k)
Wave Number, k [Å -1]
0
5
10
15

Fig.1

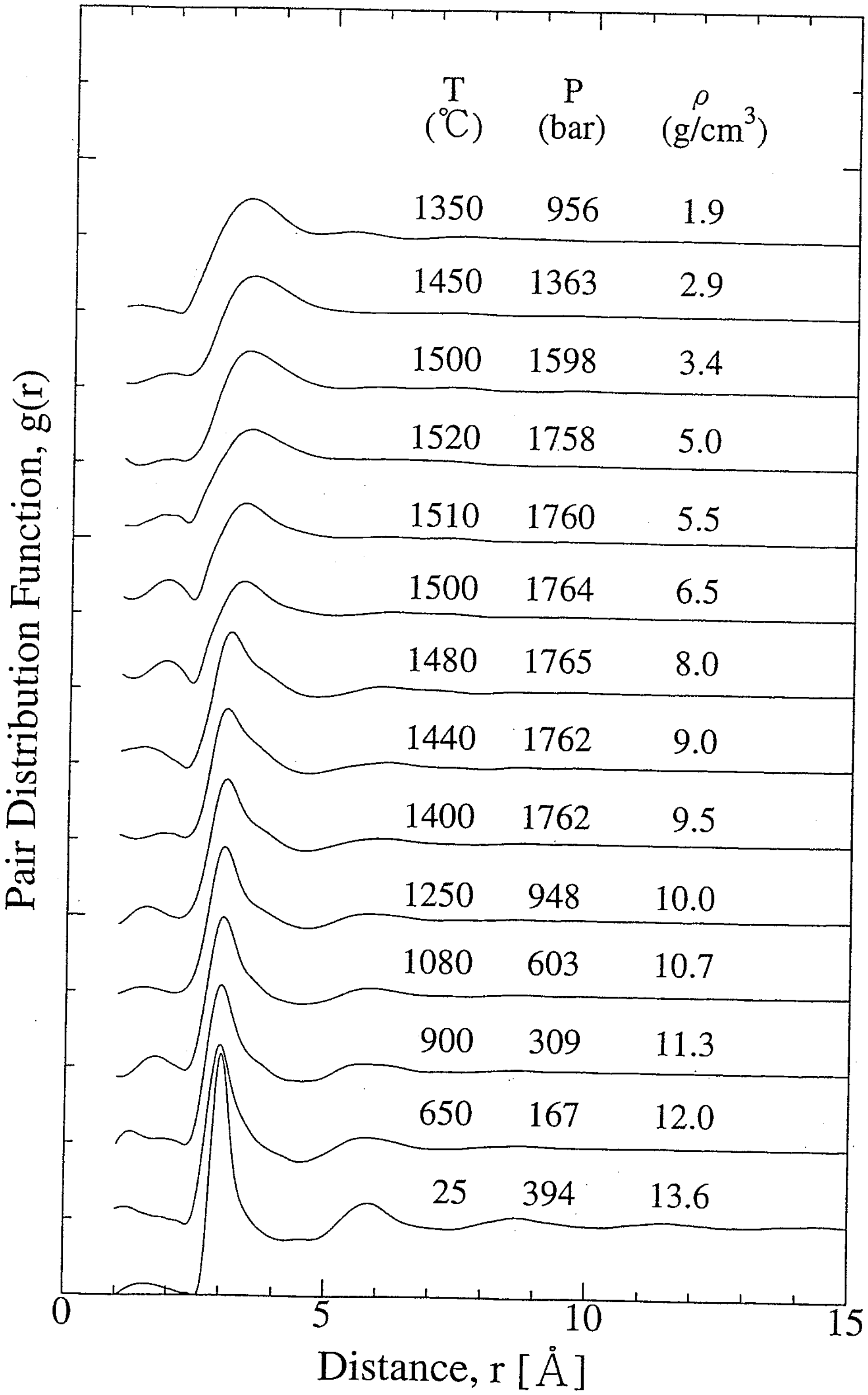
Pair Distribution Function, g(r)
T (℃)
P (bar)
ρ (g/cm³)
1350 956 1.9
1450 1363 2.9
1500 1598 3.4
1520 1758 5.0
1510 1760 5.5
1500 1764 6.5
1480 1765 8.0
1440 1762 9.0
1400 1762 9.5
1250 948 10.0
1080 603 10.7
900 309 11.3
650 167 12.0
25 394 13.6
0
5
10
15
Distance, r [Å]

Fig.2

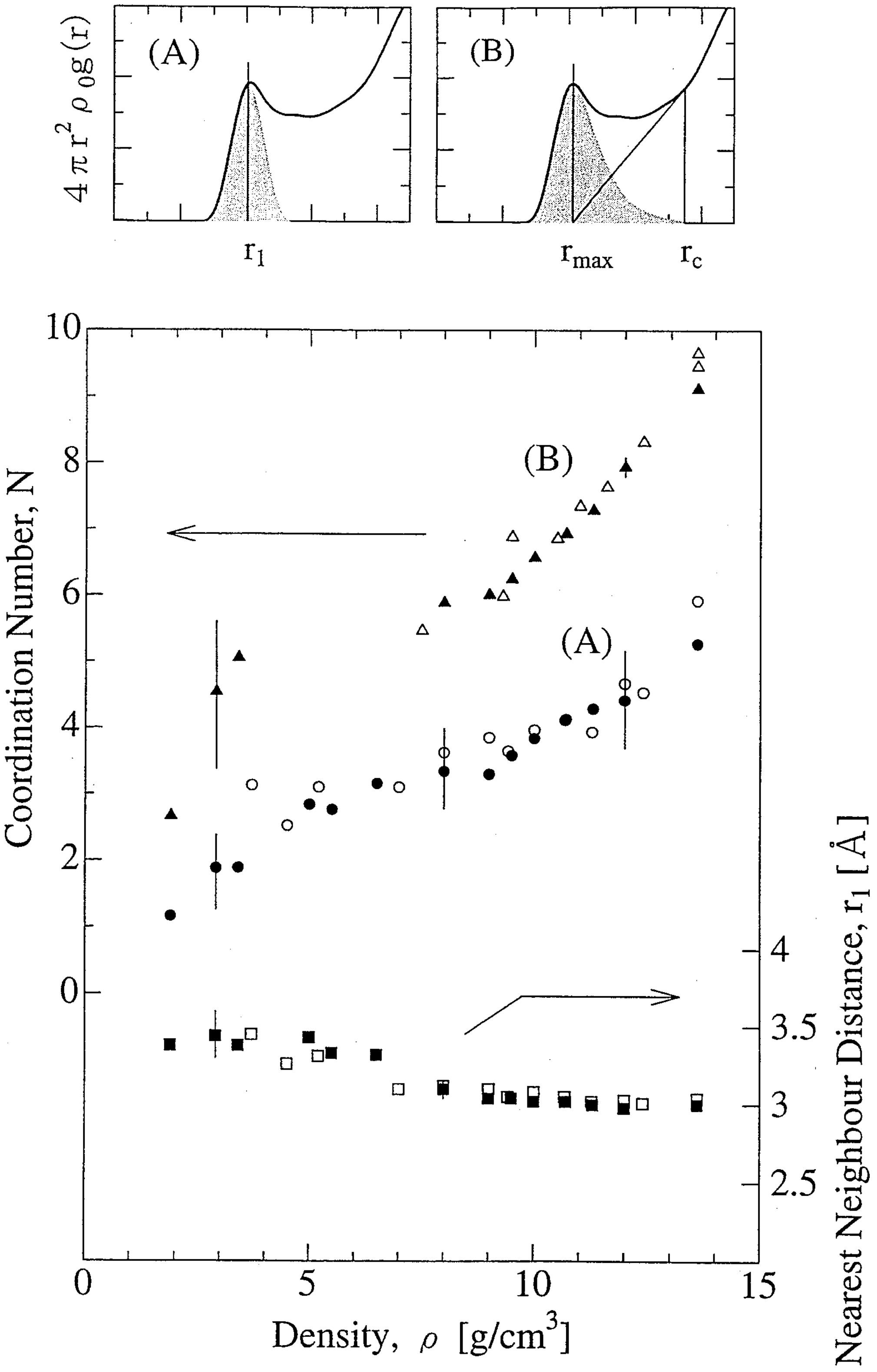
4πr²ρ₀g(r)
(A)
(B)
r₁
r_max
r_c
Coordination Number, N
Nearest Neighbour Distance, r₁ [Å]
Density, ρ [g/cm³]
(B)
(A)
0
2
4
6
8
10
0
5
10
15
2.5
3
3.5
4

Fig.3